2328–2339 *Nucleic Acids Research, 2006, Vol. 34, No. 8*
doi:10.1093/nar/gkl317

Targeting the dimerization initiation site of HIV-1 RNA with aminoglycosides: from crystal to cell

Eric Ennifar[1], Jean-Christophe Paillart[1], Anne Bodlenner[2], Philippe Walter[1], Jean-Marc Weibel[2], Anne-Marie Aubertin[3], Patrick Pale[2], Philippe Dumas[1,*] and Roland Marquet[1,*]

[1]UPR 9002 du CNRS conventionnée à l'Université Louis Pasteur, IBMC, 15 rue René Descartes, 67084, Strasbourg cedex, France, [2]UMR 7123 CNRS—Université Louis Pasteur, Institut Le Bel, 4 rue Blaise Pascal, BP 1032/F, 67070, Strasbourg cedex, France and [3]UMR 544 INSERM—Université Louis Pasteur, Institut de Virologie, 3 rue Koberlé, 67000 Strasbourg, France

Received March 15, 2006; Revised and Accepted April 12, 2006

ABSTRACT

The kissing-loop complex that initiates dimerization of genomic RNA is crucial for Human Immunodeficiency Virus Type 1 (HIV-1) replication. We showed that owing to its strong similitude with the bacterial ribosomal A site it can be targeted by aminoglycosides. Here, we present its crystal structure in complex with neamine, ribostamycin, neomycin and lividomycin. These structures explain the specificity for 4,5-disubstituted 2-deoxystreptamine (DOS) derivatives and for subtype A and subtype F kissing-loop complexes, and provide a strong basis for rational drug design. As a consequence of the different topologies of the kissing-loop complex and the A site, these aminoglycosides establish more contacts with HIV-1 RNA than with 16S RNA. Together with biochemical experiments, they showed that while rings I, II and III confer binding specificity, rings IV and V are important for affinity. Binding of neomycin, paromomycin and lividomycin strongly stabilized the kissing-loop complex by bridging the two HIV-1 RNA molecules. Furthermore, *in situ* footprinting showed that the dimerization initiation site (DIS) of HIV-1 genomic RNA could be targeted by these aminoglycosides in infected cells and virions, demonstrating its accessibility.

INTRODUCTION

Dimerization of genomic RNA is ubiquitous among retroviruses (1,2). It is beneficial for reverse transcription, including recombination, and is intricately linked to encapsidation of the genomic RNA and possibly to the morphogenesis of the mature viral core [for review, see (3)]. It was also proposed to indirectly regulate translation of the *gag* gene (3).

In Human Immunodeficiency Virus Type 1 (HIV-1), the dimerization initiation site (DIS) of the genomic RNA is a stem–loop (SL1) motif characterized by a 6 nt self-complementary sequence in a 9 nt loop. The same self-complementary sequence is found in all HIV subtypes, except in subtypes B and D, and flanking nucleotides are mostly purines (Figure 1a and b) (3). Mutations in SL1 are characterized by unstable and/or aberrant RNA dimers; they affect RNA packaging and reverse transcription, and result in strongly diminished infectivity (up to 100 000-fold) (4–7).

RNA dimerization is initiated by intermolecular base pairing of the DIS self-complementary sequence (8–11), and the resulting 'kissing-loop' complex is stabilized by the flanking unpaired nucleotides (12–14) (Figure 1c). *In vitro* studies on short RNA fragments showed that the isolated SL1 could also adopt a more stable extended duplex structure [(3) and references therein]. Inside the virions, the initial poorly stable dimer is maturated into a more stable dimer upon processing of the Gag precursor (15). However, there is no evidence that this mature dimer corresponds to the extended dimer formed *in vitro* by short RNAs (3).

These studies suggest that the kissing-loop complex formed by SL1 could be a potential target for anti-HIV-1

*To whom correspondence should be addressed. Tel: +33388417002; Fax: +33388602218; Email: P.Dumas@ibmc.u-strasbg.fr
*Correspondence may also be addressed to Roland Marquet. Tel: +33388417054; Fax: +33388602218; Email: R.Marquet@ibmc.u-strasbg.fr

The authors wish it to be known that, in their opinion, the first two authors should be regarded as joint First Authors

© The Author 2006. Published by Oxford University Press. All rights reserved.

The online version of this article has been published under an open access model. Users are entitled to use, reproduce, disseminate, or display the open access version of this article for non-commercial purposes provided that: the original authorship is properly and fully attributed; the Journal and Oxford University Press are attributed as the original place of publication with the correct citation details given; if an article is subsequently reproduced or disseminated not in its entirety but only in part or as a derivative work this must be clearly indicated. For commercial re-use, please contact journals.permissions@oxfordjournals.org

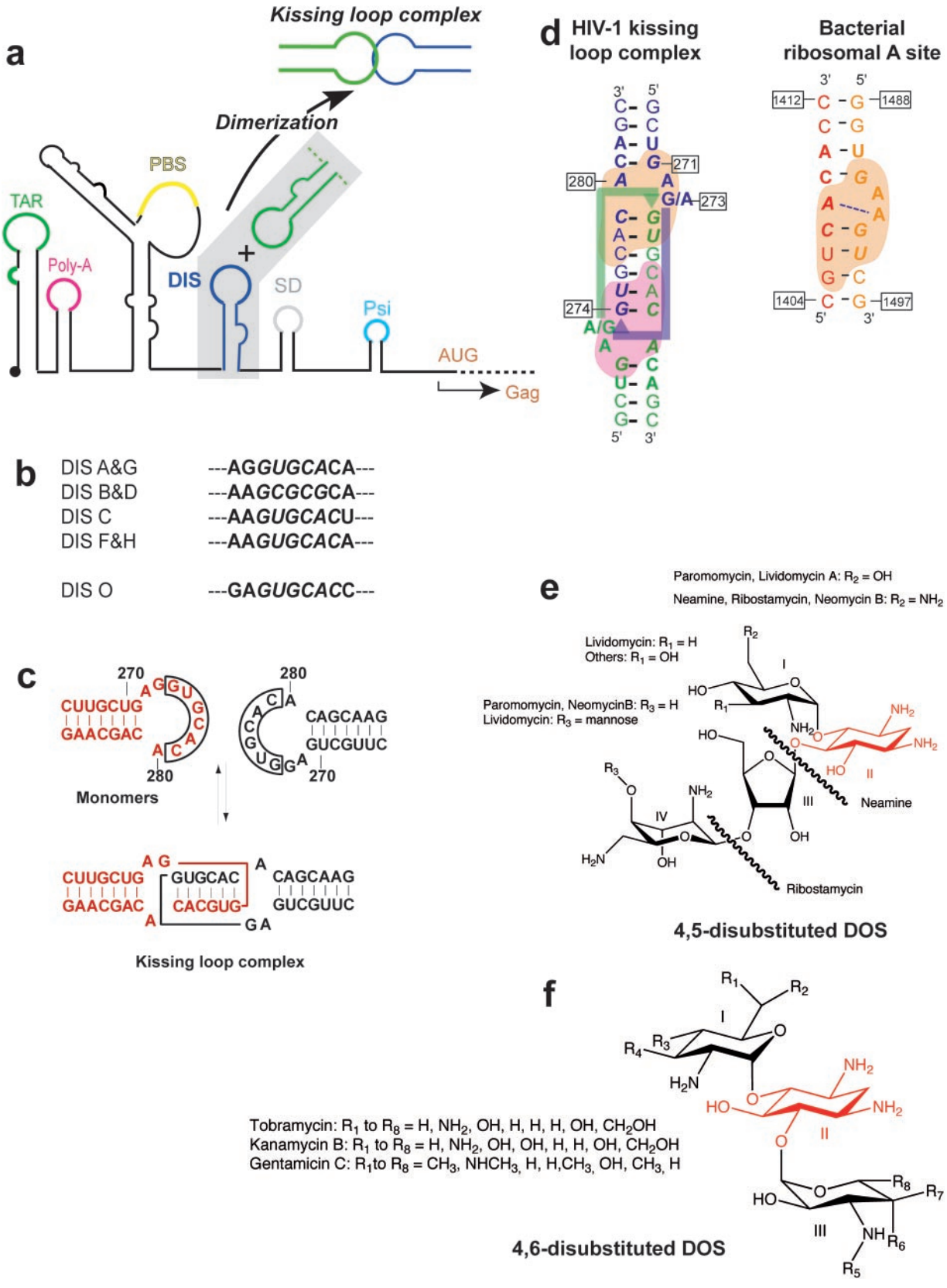

Figure 1. The HIV-1 DIS and aminoglycosides. (**a**) Location of the DIS in the 5′-untranslated region (5′-UTR) of the genomic RNA. (**b**) Phylogeny of the DIS loop. (**c**) Mechanism of dimerization. (**d**) Similitude between the DIS kissing-loop complex and the bacterial ribosomal A site. Nucleotides that are identical in the two RNAs are in boldface; those that are required for binding of aminoglycoside antibiotics to the ribosomal A site are indicated in bold italic. (**e**) 4,5-disubstituted and (**f**) 4,6-disubstituted DOS derivatives used in this study. The common DOS ring is colored in red. Note that neamine is a monosubstituted DOS.

drugs. Here, as a first step towards the development of such molecules, we studied the selective targeting of the SL1 kissing-loop complex by aminoglycosides (Figure 1e and f). Indeed, the secondary and tertiary structures of the DIS kissing-loop complex present an unexpected strong similitude with the bacterial ribosomal A site (Figure 1d), and a preliminary study showed that some, but not all, aminoglycoside antibiotics that bind to the ribosomal A site also bind to the DIS (16). Here, we present high-resolution X-ray structures of four aminoglycosides bound to the DIS kissing-loop complex. They demonstrate specific binding of neamine and 4,5-disubstituted 2-deoxystreptamine (DOS) to the DIS and provide the basis for rational design of ligands with improved properties. In addition, we were able to demonstrate that some of these aminoglycosides are able to target the DIS in the context of the genomic RNA in infected cells and in virions and that they prevent dissociation of the kissing-loop complex *in vitro*.

MATERIALS AND METHODS

Crystallization of DIS/aminoglycoside complexes

A 23mer RNA corresponding to the subtype F DIS was purchased from Dharmacon (Boulder, CO) and purified as described (17). For structure solving, a 5-bromo-uridine was substituted for uridine 3 of the 23mer RNA. RNA was heated in water at 90°C for 3 min and chilled on ice for 10 min. Buffer was then added to reach a final concentration of 150 mM KCl, 5 mM $MgCl_2$ and 20 mM sodium cacodylate (pH 7.0). RNA was then concentrated on a Centricon 10 K (Millipore) to a final concentration of 300–360 μM. All aminoglycosides were obtained from Sigma and used without purification, except neamine, which was obtained from neomycin by acidic treatment as described (18). Crystals of aminoglycoside/DIS complexes were obtained by mixing 7 μl of the RNA solution with 1.8 μl of a solution containing 5 mM neamine chloride or ribostamycin sulfate in 30% (w/v) 2,4 methylpentanediol (MPD) or with 1.0 μl of a solution containing 5 mM neomycin sulfate or 5 mM lividomycin sulfate in 30% MPD. Sitting drops were equilibrated over 2 days at 37°C against a reservoir containing 40% MPD, 300 mM KCl, 50 mM sodium cacodylate (pH 7.0), 20 mM $MgCl_2$ and crystals were transferred at 20°C for stabilization. Crystals were frozen in liquid ethane prior to data collection.

X-ray data collection, structure solution and refinement

Data were collected at 100 or 120 K on ID23-1 and ID-29 at the ESRF (Grenoble, France) or on X06SA at the SLS (Villigen, Switzerland) (Table 1 and Supplementary Table S1) and processed with the HKL package (19). The two bromide sites of the neamine–DIS complex were located with CNS (20) using the anomalous signal. The structure was solved with CNS by MAD using a three wavelength experiment (Supplementary Table S1), followed by solvent flattening with 50% solvent content. This structure was then used to solve the ribostamycin–DIS complex by molecular replacement using CNS with PC refinement, and the neomycin–DIS complex using Molrep (21) with advanced rotation function and translation function options. The lividomycin–DIS complex was solved by rigid body refinement of the neomycin–DIS complex. Molecular replacement attempts using unbound DIS kissing-loop complexes all remained unsuccessful. All structures were refined with CNS. Potassium sites were localized by anomalous difference maps using datasets of the neomycin–DIS and ribostamycin–DIS complexes collected at 1.5 or 1.65 Å wavelengths (Supplementary Table S1) to maximize the anomalous signal of the potassium ($f'' = 1.01$ ē). Occupancy of bromide in bromo-uridines was not set to 1.0 and refined due to strong radiolysis during data collection (22).

Table 1. Data collection and refinement statistics

	Neamine[a]	Ribostamycin	Neomycin	Lividomycin[a]
PDB ID	2FCX	2FCZ	2FCY	2FD0
Space group	$C222_1$	C2	$C222_1$	$C222_1$
a (Å)	27.0	112.1	27.2	27.1
b (Å)	113.4	27.2	117.8	115.3
c (Å)	95.0	106.9	94.6	95.3
β	90°	116.7°	90°	90°
Beamline	X06SA	X06SA	X06SA	X06SA
Wavelength (Å)	0.91961	0.91946	0.91946	0.91946
Resolution range (Å)	40–2.0	20–2.0	40–2.2	40–1.8
Average redundancy	6.8	3.3	4.3	6.3
Unique reflexions	18 852	18 764	7689	26 564
Completeness[b]	98.6 (92.7)	95.4 (99.2)	96.7 (90.2)	99.3 (98.7)
Rsym[b]	7.4 (27.3)	6.3 (25.6)	5.9 (23.1)	6.1 (27.3)
Average I/σ[b]	24.4 (4.0)	18.9 (5.7)	20.7 (6.4)	26.4 (3.5)
R/Rfree	26.7/29.2	23.8/25.6	23.5/25.3	24.5/24.5
Water molecules	35	208	74	90
Cations	3 K^+	4 K^+	6 K^+	4 K^+
Anions	1 Cl^-	0	1 Cl^-, 1 SO_4^{2-}	1 Cl^-
Aminoglycosides	2	4	2	2

[a]Friedel mates were processed separately.
[b]Values for last resolution shell are shown in parenthesis.

In vitro footprinting of aminoglycosides

Chemical footprinting experiments were performed on a 23mer subtype A SL1 RNA or on RNA1-615, which corresponds to nucleotides 1–615 of HIV-1 Mal genomic RNA, as described previously (16). Chemical modification was carried out either with dimethyl sulfate (DMS, Fluka) to test the accessibility of N1-A and N3-C positions or with lead acetate (Merck), which selectivity cleaves the subtype A DIS loop between the first and second nucleotides.

Infectious HIV-1 molecular clones, cell culture, transfections and infections

The HIV-1 NL4.3 molecular clone was used to generate mutant constructs with 272–280 nt (DIS loop) from the subtype A and F isolates substituted for the homologous NL4.3 region. To obtain these constructs, the QuickChange™ site-directed mutagenesis kit was used according to the manufacturer (Stratagene), using plasmid DNA pLTR5′-NL4.3 (4). The resulting mutant plasmids were digested with AatII and SphI and the AatII–SphI fragment was substituted for the homologous region of pNL4.3. Mutations were confirmed by DNA sequencing.

HeLa cell cultures and transfections were performed as described previously (23). Viral replication of wild-type

and mutant viruses was monitored by measuring RT activity in the culture supernatant of infected H9 cells.

Aminoglycoside footprinting on the HIV-1 genomic RNA in infected cells and virions

To detect the footprint of aminoglycosides on the DIS of the HIV-1 genomic RNA, five millions CEM × 174 cells were infected with equivalent amount of wild-type and mutant viruses as determined by RT activity. One hour after infection, cells were diluted in 20 ml RPMI 1640 [supplemented with 10% heat-inactivated fetal calf serum (FCS)] and cultured in the absence or in the presence of 3 mM aminoglycosides.

At 72 h after infection, CEM × 174 cells were washed twice with phosphate-buffered saline (1× PBS) and suspended in 30 µl of 1× PBS. Progeny viruses were collected and purified as described (23). Cells and viruses were treated with 3 µl of DMS for 4 and 8 min at 37°C. Reaction was stopped by adding 1 ml of TriReagent (Molecular Research Center), and RNA was extracted as described by the supplier. Modified bases were detected by primer extension as described (24).

Stabilization of the kissing-loop complex by aminoglycosides

In a typical experiment, unlabeled 1–615 RNA (400 nM), together with a corresponding internally labeled RNA (3–5 nCi), were heated for 2 min at 90°C, chilled for 2 min on ice and dimerization was initiated by addition of 2 µl of 5-fold concentrated dimerization buffer [final concentration: 50 mM sodium cacodylate (pH 7.5), 300 mM KCl, 5 mM $MgCl_2$]. After incubation at 37°C for 20 min, 100 µM of aminoglycosides were added to the RNA mixture and samples were further incubated for 15 min. Then, RNA 1–311 was added as a competitor and samples were collected at 2, 5, 10, 15, 20, 30 and 60 min and analyzed on 0.8% agarose gels [45 mM Tris–borate (pH 8.3), 01 mM $MgCl_2$] at 4°C. Gels were fixed in TCA 10%, dried, and analyzed using a BAS 2000 Bio-Imager (Fuji).

RESULTS

Crystal structures of the DIS/aminoglycoside complexes

In view of our previous results (16), we attempted to co-crystallize a 23mer RNA corresponding to the subtype F DIS with neamine and several 4,5-disubstituted and 4,6-disubstituted DOS derivatives (Figure 1e and f). We obtained co-crystals with neamine, ribostamycin, neomycin and lividomycin and the structures of these four complexes were solved at 1.8–2.2 Å resolution (Table 1). These structures are very similar and mainly differ by the size of the ligand. In all complexes, two aminoglycosides interact with the two (A-site)-like motifs of the loop–loop complex (Figure 2a and b). The average distance separating the two aminoglycosides is 4.4 Å, whereas the prediction from our previous model was 5.6 Å. RNA conformational change following ligand binding is restricted to a ribose pucker shift of G_{271} from C2′-endo in most free structures (25) to C3′-endo conformation in present structures (Supplementary Figure S1). This movement induces an opening of the aminoglycoside pocket, avoiding a steric conflict between cycle I of the aminoglycosides and G_{271} phosphate and ribose.

We recently solved the structure of an unliganded form of the subtype F kissing-loop complex in which the ribose pucker of G_{271} is C3′-endo (26). This structure is also characterized by a continuous stacking of the four bulged out purines (two in each RNA molecule) of the kissing-loop complex, contrasting with the two pairs of stacked purines separated by a gap observed in most DIS kissing-loop complexes (26). Superimposition of the structures shows that binding of 4,5-disubstituted DOS to this conformation of the kissing-loop complex also requires a structural rearrangement of the binding pocket to prevent a steric clash with phosphate 272, suggesting that aminoglycoside binding is incompatible with continuous stacking of the four bulged out purines (data not shown).

Aminoglycoside binding in the DIS pocket results in the displacement of the hexahydrated magnesium, bound to the 5′-UGCA-3′ sequence of the intermolecular helix of the unliganded kissing-loop complex, that is required for dimerization of non subtype B DIS. This displacement is obligatory because the two axial water molecules bound to O4 of U_{275} and to the magnesium are replaced by the two positively charged N1 amino groups of each DOS ring (Supplementary Figure S1). This likely explains why magnesium is dispensable for DIS dimerization in presence of aminoglycosides (data not shown).

Each aminoglycoside molecule interacts simultaneously with both RNA molecules of the loop–loop helix. Interactions are either direct, or mediated by conserved water molecules or cations (Figure 2c,d and Figure 3 and Supplementary Figure S2). Ring II (the DOS ring) almost exclusively interacts with one RNA molecule (in blue in Figure 2c,d and Figure 3), while rings I, III and IV bind only to the other RNA molecule (in green in Figure 2c,d and Figure 3). A total of 15 direct antibiotic-RNA contacts are observed for the neomycin–DIS complex (Figure 3), i.e. more than in the equivalent paromomycin–ribosomal A site complex, which is stabilized by 11 direct contacts. Analysis of these contacts reveals that, as for the A site, rings I, II and III are responsible for the sequence and structure specificity of aminoglycoside binding: base-specific contacts involve residues G_{271}, A_{278}, C_{279}, G_{274} and U_{275}, as well as A_{280} which forms a Watson–Crick-like base pair with ring I (Figure 3). Many of these contacts were also observed between this 'ribostamycin core' and the ribosomal A site. This is not surprising, given the remarkable similitude of the two complexes (Figure 4). However, some contacts are specific for the DIS–4,5-disubstituted DOS complexes: e.g. with the A_{278} of the U_{275}–A_{278} base pair replacing U_{1406} in the universal U_{1406}–U_{1495} mismatch in the ribosomal 18S RNA (Figure 1d). More interesting are the two phosphates of the bulged-out A_{1492} and A_{1493} of the ribosomal RNA that make direct contacts with O3′ and O4′ of ring I (27,28). Because of the difference in topology between the two RNA structures (loop–loop complex versus duplex), these phosphates are displaced in the DIS compared to the ribosomal A site (Figure 4). In spite of this difference, ring I is able to strongly bind to the loop–loop backbone owing to four direct interactions involving O4′, O3′ and N2′ with

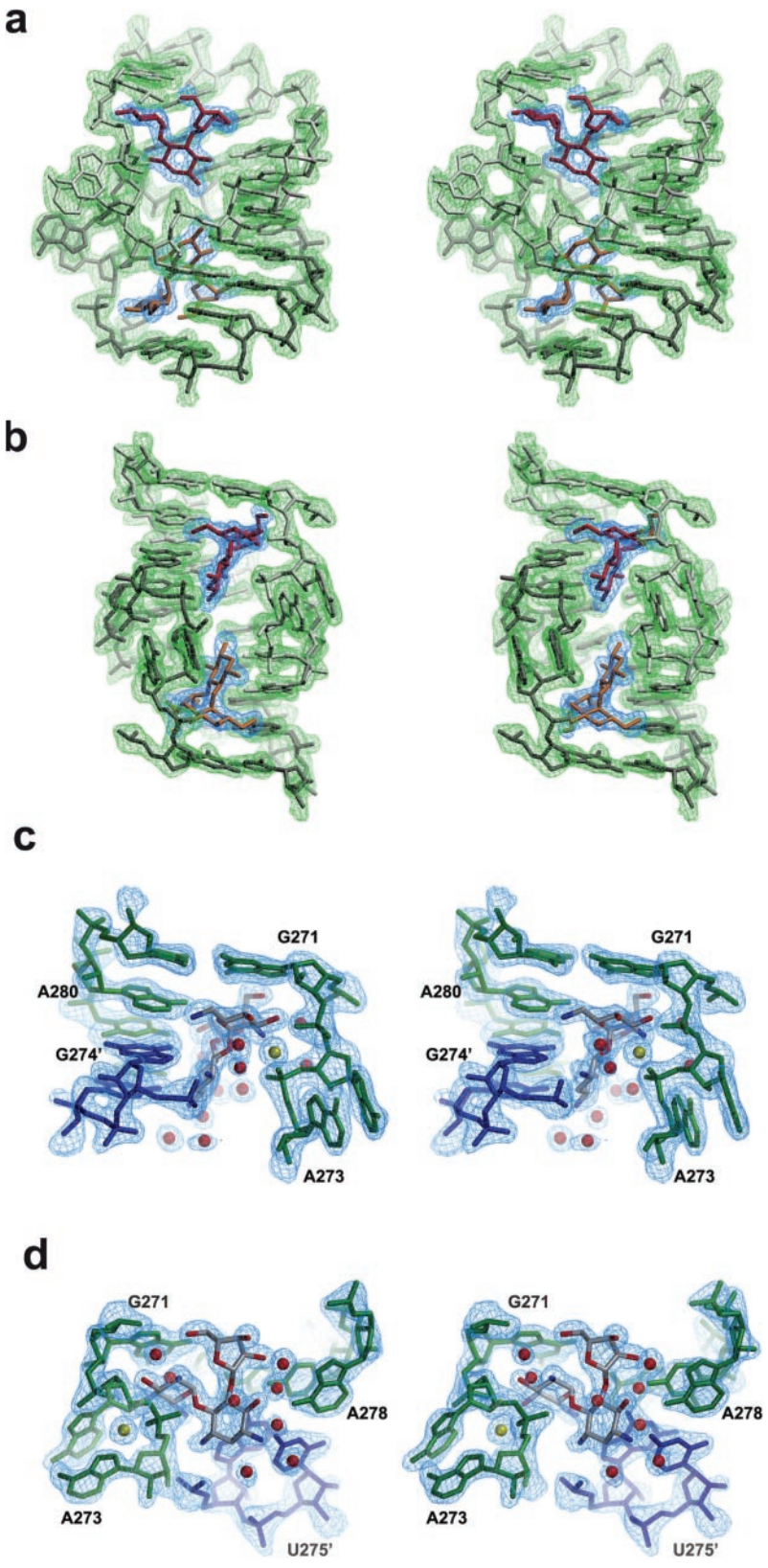

Figure 2. Structure of the ribostamycin/DIS complex. (**a** and **b**): two stereo views of the ribostamycin–DIS complex rotated by 90°. The two RNA molecules are represented in light and dark grey and the two aminoglycosides in red and orange. The 2Fo-Fc electron density map contoured at 1.4 σ level is represented in green around the RNA and in blue around aminoglycosides. For the sake of clarity, water molecules and ions are not represented. (**c** and **d**): details of the DIS–ribostamycin complex. The two RNA strands are represented in green and blue. Potassium cations and water molecules are represented as yellow and red spheres, respectively. The 2Fo-Fc electron density map contoured at 1.4 σ level is represented around the refined model.

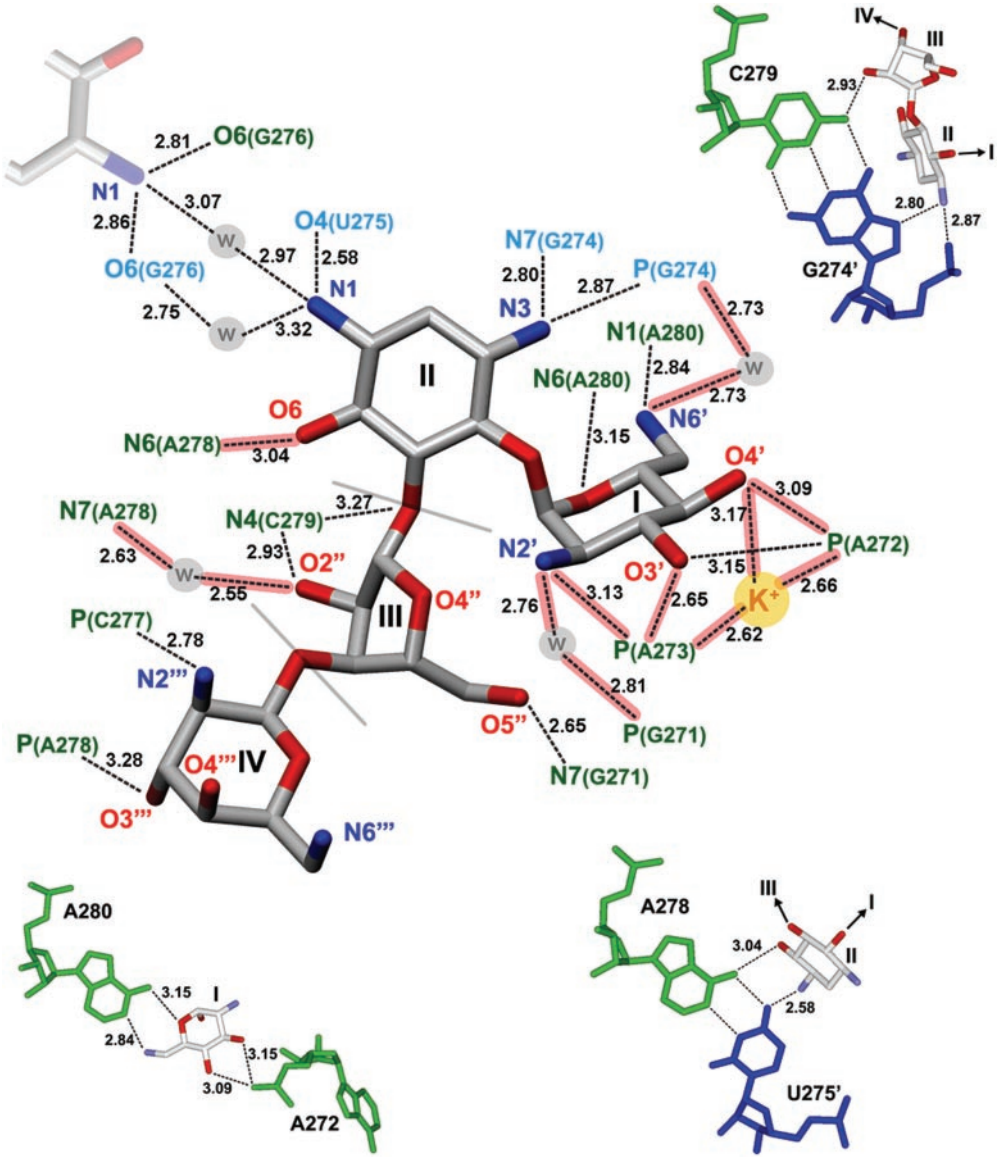

Figure 3. Schematic drawing summarizing all neomycin–RNA contacts. Contacts underlined in pink were not present in the equivalent aminoglycoside-ribosomal A site structure. 'w' and 'K^+' spheres represent water molecules and a potassium cation, respectively. The two RNA strands of the kissing-loop complex are represented and annotated in blue and in green.

the phosphate moiety of A_{272} and A_{273} (Figure 2c,d and Figure 3). In addition, the high quality of the electron density maps allowed the observation of a complex network of well-defined water molecules reinforcing the drug–RNA interaction. Water bridges were also observed between the two aminoglycoside molecules within a loop–loop complex (Figure 3 and Supplementary Figure S2). Also interesting, a conserved potassium cation was observed at the drug–RNA interface, where it mediates contacts between ring I and the phosphate group of A_{272} and A_{273} (Figure 2c,d and Figure 3 and Supplementary Figure S2). This peculiar mode of potassium binding is present neither in the unliganded DIS loop–loop complex, nor in the aminoglycoside/ribosomal A site complexes. Thus, this is a specific feature of the DIS–aminoglycoside complexes. As the O3′ hydroxyl group is lacking in lividomycin (Figure 1e), the potassium ion is not present in the DIS–lividomycin complex (Supplementary Figure S2), and direct contacts involving this position are also lost.

At variance with the 'ribostamycin core', rings IV and V bind more loosely to the DIS and are exclusively involved into non-specific interactions with the RNA backbone. These rings adopt several conformations in the RNA deep groove, and they are characterized by high temperature factors, contrasting with the very low temperature factors of rings I and II and the surrounding RNA. As a consequence, the density for ring V, and also to some extent for ring IV, is poor (Supplementary Figure S2), as also observed in the complexes with the ribosomal A site (28,29). This flexibility is confirmed by a superimposition of rings I and II of paromomycin bound to the ribosomal A site (28) to the aminoglycosides observed in the present structures

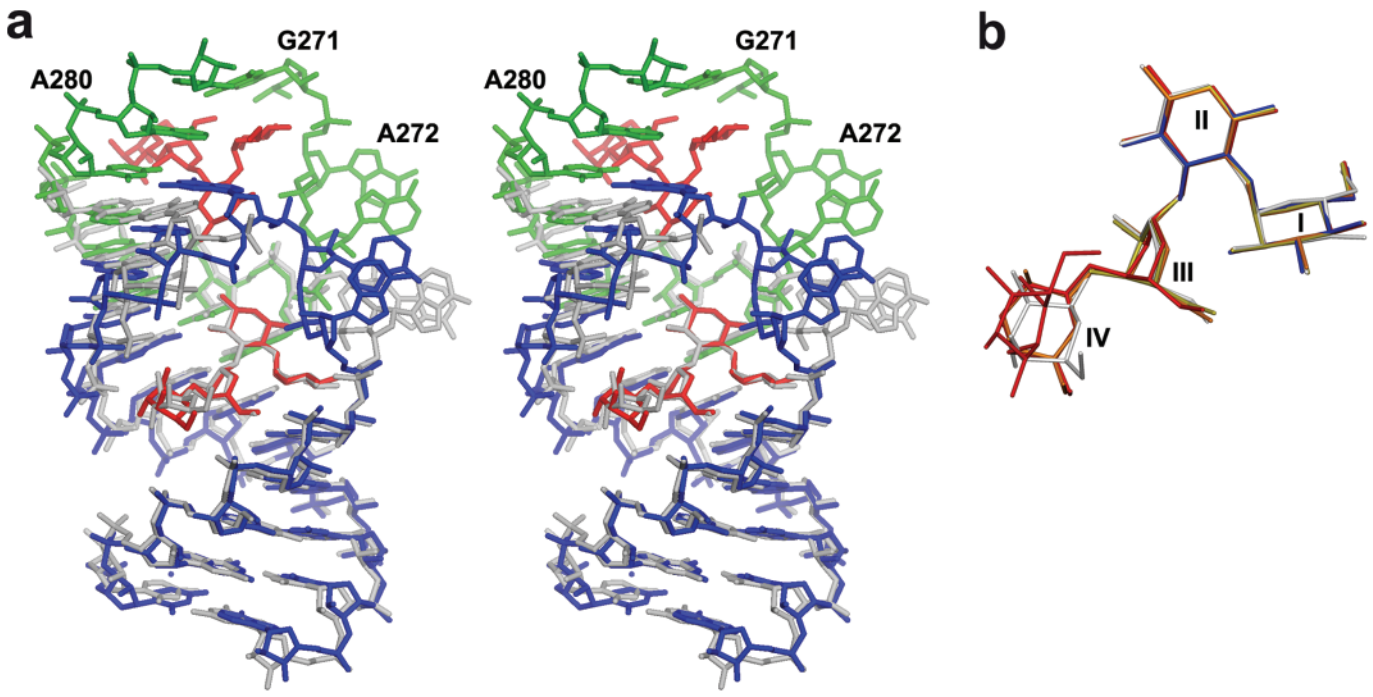

Figure 4. (**a**) Superimposition of the ribosomal A site–paromomycin complex (grey) with the DIS–neomycin complex (neomycin is in red and the two RNA molecules in blue and green). (**b**) Superimposition of paromomycin in the A site (grey) with neamine (blue), ribostamycin (yellow), neomycin (orange) and lividomycin (red) bound to the DIS loop–loop complex. Rings I to IV are labeled, whereas ring V of lividomycin, which points towards the reader, is not. The r.m.s.d. for rings I and II ranges from 0.08 to 0.25 Å.

(Figure 4). Rings I, II and III adopt a unique conformation in all structures, whereas rings IV and V (by comparing the two molecules in the asymmetric unit) can adopt different orientations.

In vitro binding of aminoglycoside antibiotics to the DIS

Even though a number of 4,5-disubstituted and 4,6-disubstituted DOS derivatives were tested, we only obtained co-crystals of the DIS kissing-loop complex with neamine and 4,5-disubstituted compounds. Indeed, all our attempts at co-crystallizing 23mer SL1 RNA with tobramycin or kanamycin B, two 4,6-disubstituted DOS (Figure 1f), resulted in crystals containing only the RNA. Modeling of 4,6-disubstituted compounds in the kissing-loop complex based on the structural analogy with the ribosomal A site and the structure of this site with tobramycin and gentamicin, suggests that these compounds would clash with positions N4 of C_{277} and N6 of A_{278} in the kissing-loop complex, where it differs from the ribosomal A site (Supplementary Figure S3). However, minor changes in the RNA structure would be sufficient to allow binding of 4,6-disubstituted DOS to the kissing-loop complex.

At this stage, it was unclear if this class of compound is able to bind to the DIS kissing-loop complex. Therefore, to compare binding of 4,5-disubstituted and 4,6-disubstituted DOS, we let a 23mer RNA corresponding to the subtype-A DIS form the kissing-loop complex. As shown previously, lead (II) induced a specific cleavage in the subtype A DIS loop that is sensitive to the binding of aminoglycoside (Figure 5a). Remarkably, none of the 4,6-disubstituted DOS we tested inhibited this cleavage at 100 μM, suggesting that they did not bind to the kissing-loop complex. Among the 4,5-disubstituted DOS, neomycin, paromomycin and lividomycin completely inhibited lead-induced cleavage of the subtype A DIS loop at 25 μM, whereas ribostamycin was less efficient (Figure 5a and data not shown). Unexpectedly, the bicyclic neamine inhibited cleavage at lower concentration than the tricyclic ribostamycin (Figure 5a). Neamine has also a higher affinity than ribostamycin for the ribosomal A site (30), but neither the crystal structures of these aminoglycosides with the DIS kissing-loop complex (this study) nor those with the ribosomal A site (29) provide a clear explanation for these observations.

In order to evaluate the capacity of neamine and 4,5-disubstituted DOS to bind to the DIS kissing-loop complex in a larger RNA presenting numerous unspecific binding sites, we used RNA1–615, which corresponds to nucleotides 1–615 of the HIV-1 MAL genomic RNA. This recombinant isolate possesses a subtype A DIS. Using a primer extension assay, we found that the lead-induced cleavage between nucleotides A_{272} and G_{273} (in this isolate, the DIS loop corresponds to nucleotides 272–280; see Figure 1c) was almost completely inhibited at 50 μM neomycin and lividomycin (Figure 5b). Similar results were obtained with paromomycin (data not shown). However, no inhibition was observed with neamine and ribostamycin, even at 100 μM (Figure 5b).

To confirm these results, we used DMS footprinting (Figure 5c). Residues A_{272} and A_{280} of RNA1–615 are unpaired in the kissing-loop complex and are methylated by DMS at their N1 position. As observed previously (13,31),

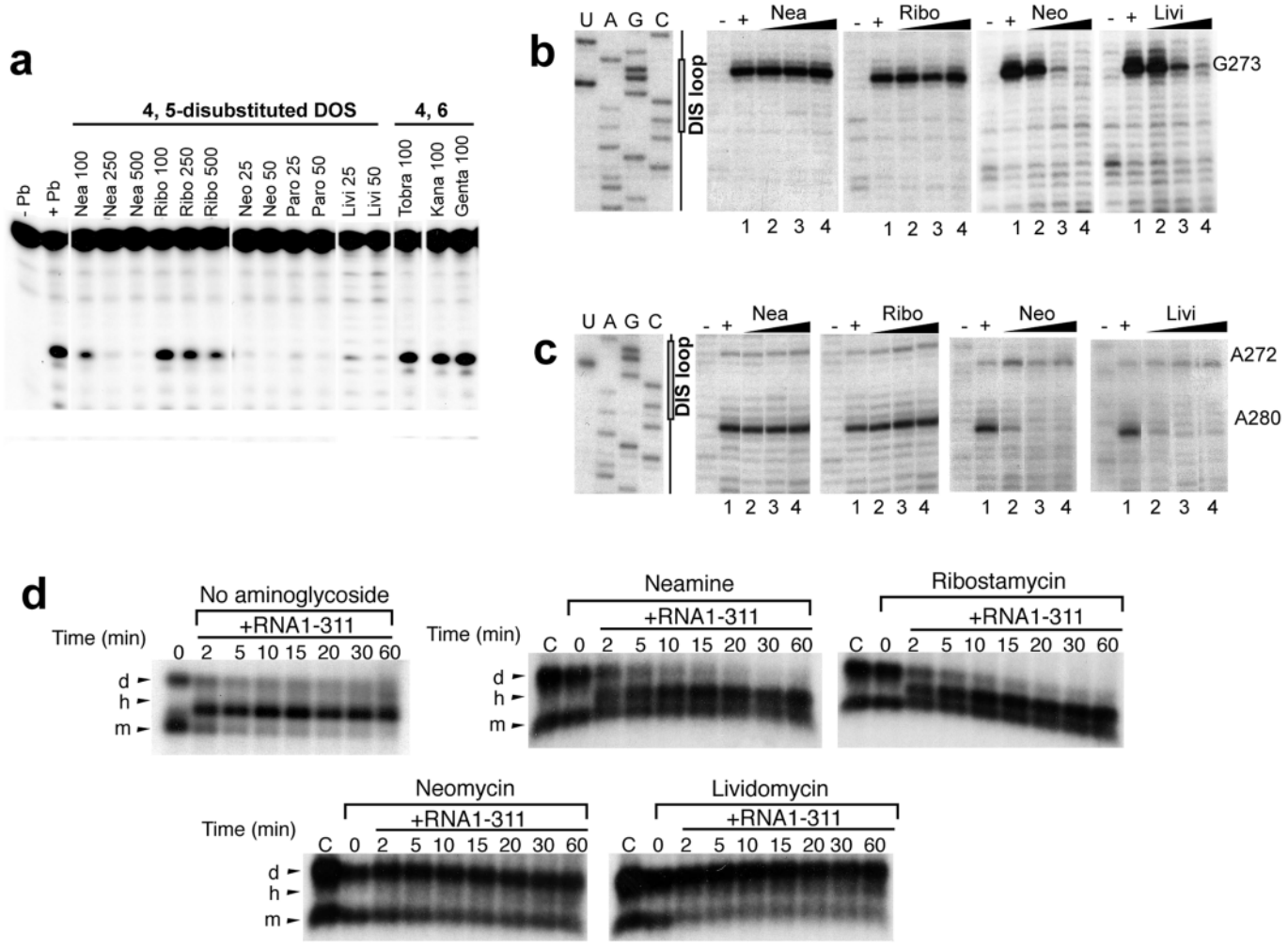

Figure 5. *In vitro* binding of aminoglycosides to subtype F and subtype A DIS. (**a**) Inhibition of the lead (II)-induced cleavage of a 23mer subtype F DIS RNA by aminoglycosides. Nea, Ribo, Neo, Paro, Livi, Tobra, Kana, Genta stand for neamine, ribostamycin, paromomycin, lividomycin, tobramycin, kanamycin and gentamicin, respectively. Numbers correspond to μM concentration of the aminoglycoside. −Pb and +Pb correspond to control lanes without aminoglycoside, without and with lead acetate, respectively. (**b**) Inhibition of lead-induced cleavage of MAL RNA1–615. Lanes 1–4 correspond to 0, 10, 50 and 100 μM aminoglycoside. (−) corresponds to an extension control performed in the absence of lead acetate. (**c**) DMS footprinting of aminoglycosides on MAL RNA1–615. Aminoglycoside concentrations and control lanes are as in (b). In (b and c), lanes U, A, C and G correspond to dideoxy sequencing reactions, which allowed to localize the lead-induced cut and methylated adenines, respectively. (**d**) Stabilization of the kissing-loop complex by 4,5-disubstituted DOS. Radiolabeled RNA 1–615 was incubated in dimerization buffer, and unlabeled RNA1–311 was added to the solution in absence or in presence of aminoglycoside, as indicated above the gel. Lane C, control dimer without aminoglycoside. d, m and h stand for dimer, monomer and heterodimer, respectively.

A_{280} is more reactive than A_{272}, even though the latter nucleotide is flipped out of the helix, while the former is stacked inside the structure. At 10 μM and above, neomycin and lividomycin strongly protected A_{280} against methylation (Figure 5c). This result was predictable in light of the pseudo-Watson–Crick interaction between this base and ring I of 4,5-disubstituted DOS (Figure 3). On the other hand, A_{272}, which is flipped out of the kissing-loop complex was not protected against methylation by DMS (Figure 5c). Importantly, A_{280} was the sole nucleotide to be protected against methylation by neomycin and lividomycin in the region covered by the primer used in this study (150–350 nt). As for the lead-induced cleavage, neamine and ribostamycin provided no protection against methylation, even at 100 μM (Figure 5c). Thus, even though these compounds bound to short DIS RNA in the same way as neomycin and lividomycin (Figure 4), they were unable to efficiently recognize this target in the context of a large RNA containing numerous unspecific binding sites.

Using DMS footprinting, we found that neomycin, paromomycin and lividomycin also efficiently bound to the subtype F kissing-loop complex in the context of RNA1–615, while neamine and ribostamycin did not (data not shown). In addition, in line with our previous study (16), none of the 4,5-disubstituted DOS bound to the subtype B kissing-loop complex (data not shown).

Stabilization of the kissing-loop complex by 4,5-disubstituted DOS

Preliminary studies on a short RNA strongly suggested that aminoglycosides increase the thermal stability of the DIS kissing-loop complex (16). Here, we directly studied the

effects of aminoglycosides on the dynamics of the kissing-loop complex at 37°C, in the context of RNA1-615 (Figure 5d).

We formed the kissing-loop complex of radiolabeled RNA1–615, then added aminoglycosides at a 100 μM concentration. Next, we added a 5-fold excess of unlabeled RNA1–311, encompassing 1–311 nt of HIV-1 MAL genomic RNA, that also contains the subtype A DIS and is thus able to form a heterodimer with RNA1–615 (Figure 5d). Due to the dynamic nature of the kissing-loop complex, in the absence of aminoglycoside, more than half of the radioactive material was shifted in the heterodimer within 2 min, and the RNA1–615 homodimer almost completely disappeared upon prolonged incubation. Similar results were obtained in the presence of 100 μM neamine and ribostamycin (Figure 5d). However, only minimal amounts of heterodimer were formed after 1 h when 100 μM neomycin, paromomycin or lividomycin were present in the reaction, and the amount of RNA1–615 homodimer remained almost constant (Figure 5d and data not shown). This observation demonstrates that 4,5-disubstituted DOS that efficiently bound to the DIS dramatically reduced dissociation of the kissing-loop complex. This observation is in keeping with our crystal structures showing that 4,5-disubstituted DOS form a bridge between the two RNA molecules (Figure 3).

Binding of aminoglycoside antibiotics to the DIS in infected cells and virions

The next step was to test if 4,5-disubstituted DOS are able to target the DIS in the context of the complete HIV-1 genomic RNA, in infected cells or in viral particles. We recently showed that it is possible to monitor modification of the HIV-1 genomic RNA by DMS in cells and in viral particles (23,24). Here, we used this technique to detect binding of 4,5-disubstituted DOS to the DIS *ex vivo*. To the best of our knowledge, this is the first example of footprinting of a small RNA ligand in cells or virions.

As all generally used HIV-1 laboratory strains are subtype B strains, we substituted subtype A or subtype F DIS loop sequences for the original subtype B DIS loop in the pNL4.3 infectious molecular clone. These substitutions did not affect replication of the mutant viruses (Supplementary Figure S4). As previously observed *in vitro*, in the absence of aminoglycoside, A_{280} was more reactive in cells and virions than A_{272} (Figure 6a). Adding neomycin, paromomycin or livodomycin to the culture medium did not completely protect A_{280} from methylation by DMS, but the intensity of the band decreased, reflecting partial protection. In order to quantify this protection, we normalized modification of A_{280} relative to A_{272}, thus correcting the intensity of the bands for variations in the amount of material used in

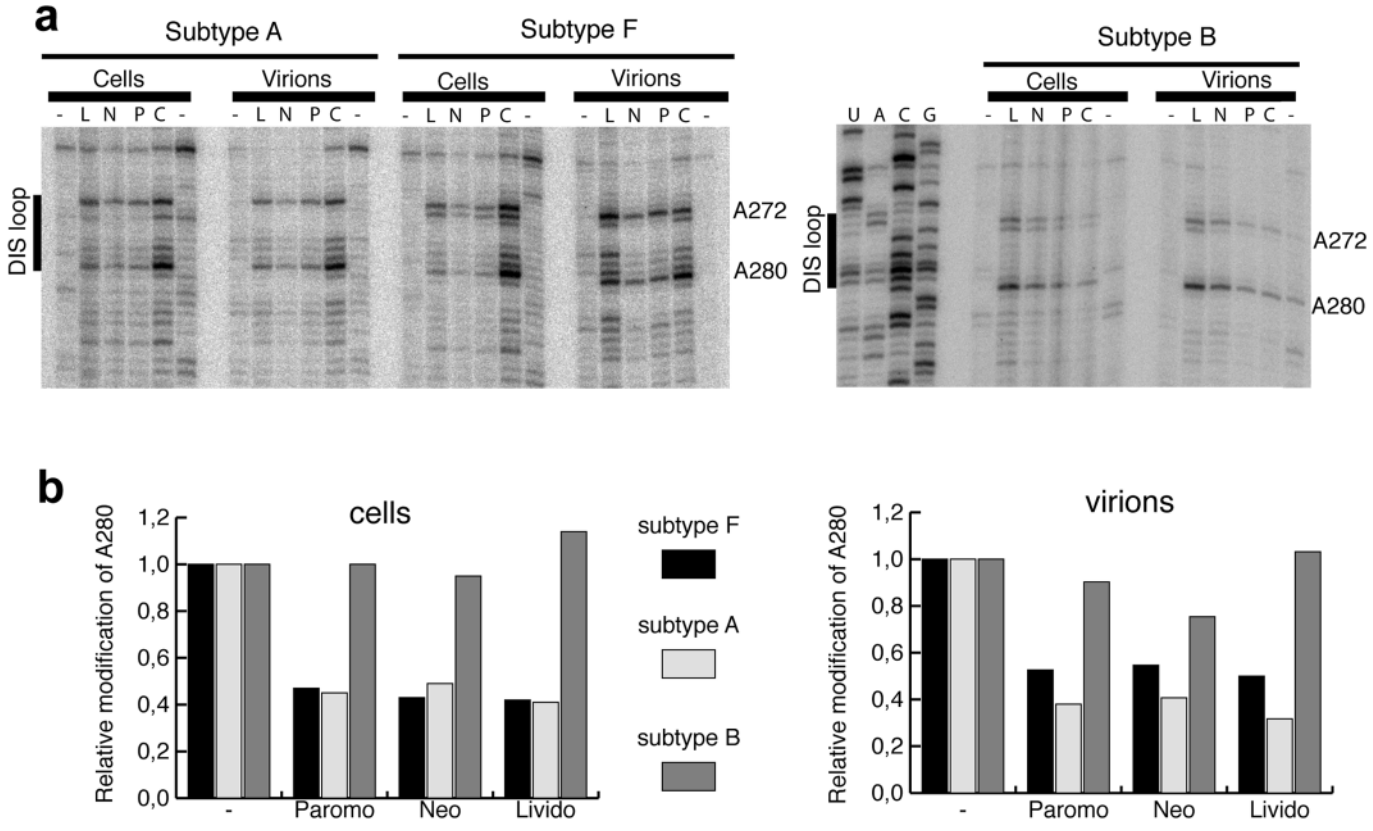

Figure 6. Aminoglycoside-induced DIS protection in CEM × 174 cells and in virions. (**a**) Methylation of the genomic RNA in infected cells and in virions was performed according to the 'Materials and Methods' section. Lane (−), extension control without DMS ; lane C, DMS treatment without aminoglycoside; lanes L, N and P: DMS treatment in the presence of lividomycin, neomycin and paromomycin, respectively. Sequence lanes (U, A, C and G) were run in parallel to identify the modified nucleotides. (**b**) The gels shown in A were quantified and modification of A_{280}, normalized to that of A_{272}, was compared to that obtained in the absence of aminoglycoside (which was arbitrarily set to 1 for each HIV-1 subtype).

the primer extension assay. The influence of aminoglycosides on the relative modification of A_{280} is shown in Figure 6b. Paromomycin, neomycin and lividomycin did not protect A_{280} against methylation of subtype B DIS in infected cells and in viral particles. However, these three 4,5-disubstituted DOS reduced alkylation of the subtype A and subtype F DIS more than 2-fold. Subtype A and subtype F DIS were protected to the same extent in cells, while protection of subtype F DIS was systematically more efficient in virions (Figure 6b). The origin of this difference is unknown. Notably, paromomycin, neomycin and lividomycin provided similar levels of protection. As already noticed in our *in vitro* experiments, A_{280} was the sole nucleotide to be protected against DMS by paromomycin, neomycin and lividomycin in cells and virions in the region we analyzed (150–350 nt).

DISCUSSION

Despite the efficiency of highly active antiretroviral therapy, the emergence of resistant strains and the side effects of the current treatments highlight the need for new inhibitors of HIV-1 replication. In addition to viral and cellular proteins, the genomic RNA itself has been proposed as a drug target (32). For instance, molecules targeting the trans activating region (TAR) (33–35), the packaging signal (36,37), the frameshifting signal (38) and the rev responsive element (RRE) (39,40) have been selected *in vitro*. Aminoglycosides have been shown to bind to several of these sites (34,36,37,39,40), but in most cases, the selectivity and specificity of binding were not addressed or poorly understood.

We took advantage of the structural similitude we identified between the crystal structures of the bacterial ribosomal A site and the HIV-1 kissing-loop complex (16) to target the DIS with aminoglycosides that are known to specifically interact with the bacterial A site. Indeed, binding of aminoglycosides to the kissing-loop complex could be predicted from its crystal structure, characterized by the first two purines of the DIS loop bulging out (25), but not from its NMR structures (41,42), in which one or two of these purines are buried in the structure. The crystal structures of the DIS–aminoglycoside complexes we report here confirm the strong similitude of the kissing-loop complex with the ribosomal A site, and support the biological relevance of the flipped out conformation of the first two purines of the DIS loop. Strangely enough, several contacts are specific for the kissing-loop complex, and 4,5-disubstituted DOS build more direct interactions with the kissing-loop complex than with the A site.

Interestingly, our crystal structures and biochemical experiments revealed that binding of aminoglycosides to the DIS is specific regarding both the aminoglycoside family and the RNA subtype. In contrast with neamine and 4,5-disubstituted DOS, 4,6-disubstituted DOS, which also bind to the bacterial ribosomal A site, do not specifically bind to the HIV-1 kissing-loop complex. Our crystal structures combined with modeling strongly suggest that residue A_{278} prevents binding of 4,6-disubstituted DOS to the kissing-loop complex. Indeed, the structurally equivalent position in the ribosomal A site is U_{1406} (Figure 1d), and it has been shown that substituting an A for U_{1406} in the 16 ribosomal RNA confers resistance to 4,6-disubstituted DOS, but not to 4,5-disubstituted DOS (43,44).

Neamine and 4,5-disubstituted DOS bind to subtype A and subtype F, but not to subtype B DIS. Our X-ray structures of the subtype F DIS complexed with neamine and 4,5-disubstituted DOS demonstrate that this subtype specificity is linked to the identity of the second nucleotide in the DIS self-complementary sequence. This nucleotide is a uridine (U_{275}) in all HIV-1 subtypes, except in subtypes B and D (Figure 1b). The corresponding nucleotide in the bacterial ribosomal A site is also a uridine (U_{1495}) (Figure 1d). In the complexes involving the subtype F DIS and neamine or 4,5-disubstituted DOS, atom O4 of U_{275} makes a hydrogen bond with the amino group at position 1 of ring II of the aminoglycoside (Figure 3). In the subtype B kissing-loop complex, the amino group at position 4 of C_{275} would clash with the aminoglycoside amino group, thus preventing binding. In line with this interpretation, substituting a C or an A, but not a G, for U_{1495} in the *Escherichia coli* A site RNA prevents paromomycin binding (45), whereas substituting a C residue for U_{1495} in *Mycobacterium smegmatis* 16S RNA confers resistance to both 4,5-disubstituted and 4,6-disubstituted aminoglycosides (43). Interestingly, our crystal structures indicate that substituting a hydroxyl for the amino group at position 1 of ring II of 4,5-disubstituted DOS should allow to target subtype B HIV-1 strains.

Even though this has not been experimentally tested, our structures predict that 4,5-disubstituted DOS should not bind to the kissing-loop complex of HIV-1 strains belonging to subtype C of group M (main) and to group O (outlier). In these strains, A_{280}, which forms a pseudo Watson–Crick base pair with the aminoglycoside ring I (Figure 3), is replaced by a uridine or a cytosine, respectively (Figure 1b). If these residues are unpaired and stacked inside the structure, as A_{280} in the kissing-loop structure of subtypes A&G, B&D and F&H, it should be possible to modify ring I in order to specifically target these strains. However, in these strains, nt A280 can potentially form a Watson–Crick base pair with residue 272, reducing the DIS loop to 7 nt. If this base pair does form, it would be impossible to target the corresponding kissing-loop complexes with 4,5-disubstituted aminoglycosides. Thus, it would be interesting to solve the structure of these kissing-loop complexes.

The selectivity of binding with respect to the aminoglycoside family and to the HIV-1 subtype clearly show that binding of neamine and 4,5-disubstituted DOS to the HIV-1 kissing-loop complex does not only rely on non specific electrostatic interactions, but also on specific contacts. Our crystal structures clearly indicate that the binding specificity is mainly driven by rings I and II, and to a lesser extend by ring III of 4,5-disubstituted DOS, which interact with the RNA bases and the particular sugar-phosphate backbone motif of the kissing-loop complex. At the opposite, rings IV and V mainly contribute to binding by interacting with phosphate groups in a regular A type conformation. However, our biochemical experiments demonstrate that these interactions are essential to target the DIS when multiple non-specific targets are also present.

Indeed, our *in situ* footprinting experiments demonstrated that 4,5-disubstituted DOS with four or five rings are able to target the DIS in infected cells and in virions. These

experiments demonstrate that the DIS is accessible *in vivo*, a prerequisite for a drug target. This is the first demonstration that aminoglycosides specifically bind to HIV-1 genomic RNA in cell culture, and to the best of our knowledge, the only direct demonstration that a small ligand directed against HIV-1 RNA does bind to its predicted target in infected cells and/or in viral particles.

Binding of 4,5-disubstituted DOS to the DIS appears to stabilize the kissing-loop complex. This is not surprising since these compounds were predicted to bind to the kissing-loop complex rather than to the monomeric form of the DIS. At odds with our results, neomycin and paromomycin were also reported to bind to the subtype B DIS loop under ionic conditions in which the monomeric form of HIV-1 RNA prevails (36,37). However, as these experiments were conducted at very low ionic strength and in the absence of multivalent cations, this binding was most likely driven by unspecific electrostatic interactions, in keeping with the numerous binding sites observed in the HIV-1 packaging signal under these conditions (36,37). In line with this interpretation, our *in vitro* and *in situ* DMS footprinting experiments identified the DIS as the only specific aminoglycoside binding site between 150 and 350 nt.

Our study demonstrates that aminoglycosides can specifically target the DIS of the HIV-1 genomic RNA in cells and in virions. The next step would be to achieve inhibition of HIV-1 replication. Analysis of the effects of aminoglycosides on HIV-1 molecular clones harboring either a subtype B, a subtype A or a subtype F DIS did not show any significant inhibition that could be correlated to binding of these compounds to the DIS (J.-C. Paillart and R. Marquet, unpublished data). The lack of inhibition might be due to incomplete saturation of the DIS by aminoglycosides in cells and virions, as indicated by the partial protection of A_{280} against methylation, which is most likely the result of the poor penetration of aminoglycosides in eukaryotic cells. Alternatively, targeting and stabilizing the DIS is not sufficient to inhibit HIV-1 replication. Hopefully, our high-resolution structures of DIS–aminoglycoside complexes provide us with the necessary basis to identify aminoglycoside mimics with simpler chemistry and improved biodisponibility that would make similar interactions with the kissing-loop complex. They should also reveal invaluable for the rational design of derivatized molecules that would irreversibly cleave, crosslink or modify the viral RNA after binding to the DIS.

SUPPLEMENTARY DATA

Supplementary Data are available at NAR Online.

ACKNOWLEDGEMENTS

The authors are grateful to Chantal and Bernard Ehresmann for their constant support during this work. The authors are also grateful to the staff of the Joint Structural Biology Group at the ESRF and to Clemens Schulze-Briese and Ehmke Pohl from SLS for their excellent support. The authors thank Catherine Isel for critical reading of this manuscript. This work was supported by grants from the Agence Nationale de Recherches sur le SIDA (ANRS) to P.D. and R.M. Funding to pay the Open Access publication charges for this article was provided by ANRS.

Conflict of interest statement. None declared

REFERENCES

1. Kung,H.J., Hu,S., Bender,W., Bailey,J.M., Davidson,N., Nicolson,M.O. and McAllister,R.M. (1976) RD-114, baboon, and woolly monkey viral RNAs compared in size and structure. *Cell*, **7**, 609–620.
2. Paillart,J.C., Marquet,R., Skripkin,E., Ehresmann,C. and Ehresmann,B. (1996) Dimerization of retroviral genomic RNAs: structural and functional implications. *Biochimie*, **78**, 639–653.
3. Paillart,J.C., Shehu-Xhilaga,M., Marquet,R. and Mak,J. (2004) Dimerization of retroviral RNA genomes: an inseparable pair. *Nature Rev. Microbiol.*, **2**, 461–472.
4. Paillart,J.-C., Berthoux,L., Ottmann,M., Darlix,J.-L., Marquet,R., Ehresmann,B. and Ehresmann,C. (1996) A dual role of the putative RNA dimerization initiation site of human immunodeficiency virus type 1 in genomic RNA packaging and proviral DNA synthesis. *J. Virol.*, **70**, 8348–8354.
5. Berkhout,B. and van Wamel,J.L.B. (1996) Role of the DIS hairpin in replication of human immunodeficiency virus type 1. *J. Virol.*, **70**, 6723–6732.
6. Shen,N., Jette,L., Liang,C., Wainberg,M.A. and Laughrea,M. (2000) Impact of human immunodeficiency virus type 1 RNA dimerization on viral infectivity and of stem–loop B on RNA dimerization and reverse transcription and dissociation of dimerization from packaging. *J. Virol.*, **74**, 5729–5735.
7. Clever,J.L. and Parslow,T.G. (1997) Mutant human immunodeficiency virus type 1 genomes with defects in RNA dimerization or encapsidation. *J. Virol.*, **71**, 3407–3414.
8. Skripkin,E., Paillart,J.C., Marquet,R., Ehresmann,B. and Ehresmann,C. (1994) Identification of the primary site of human immunodeficiency virus type 1 RNA dimerization *in vitro*. *Proc. Natl Acad. Sci. USA*, **91**, 4945–4949.
9. Paillart,J.-C., Skripkin,E., Ehresmann,B., Ehresmann,C. and Marquet,R. (1996) A loop–loop 'kissing' complex is the essential part of the dimer linkage of genomic HIV-1 RNA. *Proc. Natl Acad. Sci. USA*, **93**, 5572–5577.
10. Muriaux,D., Girard,P.-M., Bonnet-Mathonière,B. and Paoletti,J. (1995) Dimerization of HIV-1Lai RNA at low ionic strength. An autocomplementary sequence in the 5′ leader region is evidenced by an antisense oligonucleotide. *J. Biol. Chem.*, **270**, 8209–8216.
11. Laughrea,M. and Jetté,L. (1994) A 19-nucleotide sequence upstream of the 5′ major splice donor is part of the dimerization domain of human immunodeficiency virus 1 genomic RNA. *Biochemistry*, **33**, 13464–13474.
12. Clever,J.L., Wong,M.L. and Parslow,T.G. (1996) Requirements for kissing-loop-mediated dimerization of human immunodeficiency virus RNA. *J. Virol.*, **70**, 5902–5908.
13. Paillart,J.C., Westhof,E., Ehresmann,C., Ehresmann,B. and Marquet,R. (1997) Non-canonical interactions in a kissing loop complex: the dimerization initiation site of HIV-1 genomic RNA. *J. Mol. Biol.*, **270**, 36–49.
14. Lodmell,J.S., Ehresmann,C., Ehresmann,B. and Marquet,R. (2000) Convergence of natural and artificial evolution on a RNA loop-loop interaction: the HIV-1 dimerization initiation site. *RNA*, **6**, 1267–1276.
15. Fu,W., Gorelick,R.J. and Rein,A. (1994) Characterization of human immunodeficiency virus type 1 dimeric RNA from wild-type and protease-defective virions. *J. Virol.*, **68**, 5013–5018.
16. Ennifar,E., Paillart,J.C., Marquet,R., Ehresmann,B., Ehresmann,C., Dumas,P. and Walter,P. (2003) HIV-1 RNA dimerization initiation site is structurally similar to the ribosomal A site and binds aminoglycoside antibiotics. *J. Biol. Chem.*, **278**, 2723–2730.
17. Ennifar,E., Walter,P. and Dumas,P. (2003) A crystallographic study of the binding of 13 metal ions to two related RNA duplexes. *Nucleic Acids Res.*, **31**, 2671–2682.
18. Park,W.K.C., Auer,M., Jaksche,H. and Wong,C.H. (1996) Rapid combinatorial synthesis of aminoglycoside antibiotic mimetics: use of a polyethylene glycol-linked amine and a neamine-derived aldehyde in multiple component condensation as a strategy for the discovery of new

inhibitors of the HIV RNA rev responsive element. *J. Am. Chem. Soc.*, **118**, 10150–10155.
19. Otwinowski,Z. and Minor,W. (1996) Processing of X-ray diffraction data collected in oscillation mode. In Carter,C.W.,Jr. and Sweet,R.M. (eds), *Methods in Enzymology*. Academic Press, Vol. **276**, pp. 307–326.
20. Brunger,A.T., Adams,P.D., Clore,G.M., DeLano,W.L., Gros,P., Grosse-Kunstleve,R.W., Jiang,J.S., Kuszewski,J., Nilges,M., Pannu,N.S. *et al.* (1998) Crystallography & NMR system: a new software suite for macromolecular structure determination. *Acta. Crystallogr. D. Biol. Crystallogr.*, **54**, 905–921.
21. Vagin,A.A. and Isupov,M.N. (2001) Spherically averaged phased translation function and its application to the search for molecules and fragments in electron-density maps. *Acta. Crystallogr. D. Biol. Crystallogr.*, **57**, 1451–1456.
22. Ennifar,E., Carpentier,P., Pirocchi,M., Walter,P., Ferrer,J. and Dumas,P. (2002) X-ray-induced debromination of nucleic acids at the Br K-absorption edge and implications on MAD-phasing. *Acta. Crystallogr. D. Biol. Crystallogr.*, **58**, 1262–1268.
23. Goldschmidt,V., Paillart,J.C., Rigourd,M., Ehresmann,B., Aubertin,A.M., Ehresmann,C. and Marquet,R. (2004) Structural variability of the initiation complex of HIV-1 reverse transcription. *J. Biol. Chem.*, **279**, 35923–35931.
24. Paillart,J.C., Dettenhofer,M., Yu,X.F., Ehresmann,C., Ehresmann,B. and Marquet,R. (2004) First snapshots of the HIV-1 RNA structure in infected cells and in virions. *J. Biol. Chem.*, **279**, 48397–48403.
25. Ennifar,E., Walter,P., Ehresmann,B., Ehresmann,C. and Dumas,P. (2001) Crystal structures of coaxially stacked kissing complexes of the HIV-1 RNA dimerization initiation site. *Nature Struct. Biol.*, **8**, 1064–1068.
26. Ennifar,E. and Dumas,P. (2006) Polymorphism of bulged-out residues in HIV-1 RNA DIS kissing-complex and structure comparison with solution studies. *J. Mol. Biol.*, **356**, 771–782.
27. Carter,A.P., Clemons,W.M., Brodersen,D.E., Morgan-Warren,R.J., Wimberly,B.T. and Ramakrishnan,V. (2000) Functional insights from the structure of the 30S ribosomal subunit and its interactions with antibiotics. *Nature*, **407**, 340–348.
28. Vicens,Q. and Westhof,E. (2001) Crystal structure of paromomycin docked into the eubacterial ribosomal decoding A site. *Structure*, **9**, 647–658.
29. Francois,B., Russell,R.J., Murray,J.B., Aboul-ela,F., Masquida,B., Vicens,Q. and Westhof,E. (2005) Crystal structures of complexes between aminoglycosides and decoding A site oligonucleotides: role of the number of rings and positive charges in the specific binding leading to miscoding. *Nucleic Acids Res.*, **33**, 5677–5690.
30. Wong,C.H., Hendrix,M., Priestley,E.S. and Greenberg,W.A. (1998) Specificity of aminoglycoside antibiotics for the A-site of the decoding region of ribosomal RNA. *Chem. Biol.*, **5**, 397–406.
31. Baudin,F., Marquet,R., Isel,C., Darlix,J.L., Ehresmann,B. and Ehresmann,C. (1993) Functional sites in the 5′ region of human immunodeficiency virus type-1 RNA form defined structural domains. *J. Mol. Biol.*, **229**, 382–397.
32. Wilson,W.D. and Li,K. (2000) Targeting RNA with small molecules. *Curr. Med. Chem.*, **7**, 73–98.
33. Hamy,F., Felder,E.R., Heizmann,G., Lazdins,J., Aboul-ela,F., Varani,G., Karn,J. and Klimkait,T. (1997) An inhibitor of the Tat/TAR RNA interaction that effectively suppresses HIV-1 replication. *Proc. Natl Acad. Sci. USA*, **94**, 3548–3553.
34. Wang,S., Huber,P.W., Cui,M., Czarnik,A.W. and Mei,H.Y. (1998) Binding of neomycin to the TAR element of HIV-1 RNA induces dissociation of Tat protein by an allosteric mechanism. *Biochemistry*, **37**, 5549–5557.
35. Hwang,S., Tamilarasu,N., Kibler,K., Cao,H., Ali,A., Ping,Y.H., Jeang,K.T. and Rana,T.M. (2003) Discovery of a small molecule Tat-trans-activation-responsive RNA antagonist that potently inhibits human immunodeficiency virus-1 replication. *J. Biol. Chem.*, **278**, 39092–39103.
36. McPike,M.P., Sullivan,J.M., Goodisman,J. and Dabrowiak,J.C. (2002) Footprinting, circular dichroism and UV melting studies on neomycin B binding to the packaging region of human immunodeficiency virus type-1 RNA. *Nucleic Acids Res.*, **30**, 2825–2831.
37. McPike,M.P., Goodisman,J. and Dabrowiak,J.C. (2002) Footprinting and circular dichroism studies on paromomycin binding to the packaging region of human immunodeficiency virus type-1. *Bioorg. Med. Chem.*, **10**, 3663–3672.
38. Hung,M., Patel,P., Davis,S. and Green,S.R. (1998) Importance of ribosomal frameshifting for human immunodeficiency virus type 1 particle assembly and replication. *J. Virol.*, **72**, 4819–4824.
39. Wang,Y., Hamasaki,K. and Rando,R.R. (1997) Specificity of aminoglycoside binding to RNA constructs derived from the 16S rRNA decoding region and the HIV-RRE activator region. *Biochemistry*, **36**, 768–779.
40. Zapp,M.L., Stern,S. and Green,M.R. (1993) Small molecules that selectively block RNA binding of HIV-1 Rev protein inhibit Rev function and viral production. *Cell*, **74**, 969–978.
41. Kieken,F., Paquet,F., Brule,F., Paoletti,J. and Lancelot,G. (2006) A new NMR solution structure of the SL1 HIV-1Lai loop-loop dimer. *Nucleic Acids Res.*, **34**, 343–352.
42. Baba,S., Takahashi,K., Noguchi,S., Takaku,H., Koyanagi,Y., Yamamoto,N. and Kawai,G. (2005) Solution RNA structures of the HIV-1 dimerization initiation site in the kissing-loop and extended-duplex dimers. *J. Biochem. (Tokyo)*, **138**, 583–592.
43. Pfister,P., Hobbie,S., Vicens,Q., Bottger,E.C. and Westhof,E. (2003) The molecular basis for A-site mutations conferring aminoglycoside resistance: relationship between ribosomal susceptibility and X-ray crystal structures. *Chembiochem.*, **4**, 1078–1088.
44. Recht,M.I. and Puglisi,J.D. (2001) Aminoglycoside resistance with homogeneous and heterogeneous populations of antibiotic-resistant ribosomes. *Antimicrob. Agents Chemother.*, **45**, 2414–2419.
45. Recht,M.I., Fourmy,D., Blanchard,S.C., Dahlquist,K.D. and Puglisi,J.D. (1996) RNA sequence determinants for aminoglycoside binding to an A-site rRNA model oligonucleotide. *J. Mol. Biol.*, **262**, 421–436.